A MEMS/NEMS sensor for human skin temperature measurement

Hongjie Leng and Yingzi Lin*

Department of Mechanical & Industrial Engineering, Northeastern University, Boston, USA

Abstract. Human state in human-machine systems highly affects the overall system performance, and should be detected and monitored. Physiological cues are essential indicators of human state and useful for the purpose of monitoring. The study presented in this paper was focused on developing a bio-inspired sensing system, i.e., Nano-Skin, to non-intrusively measure physiological cues on human-machine contact surfaces to detect human state. The paper is presented in three parts. The first part is to analyze the relationship between human state and physiological cues, and to introduce the conceptual design of Nano-Skin. Generally, heart rate, skin conductance, skin temperature, operating force, blood alcohol concentration, sweat rate, and electromyography are closely related with human state. They can be measured through human-machine contact surfaces using Nano-Skin. The second part is to discuss the technologies for skin temperature measurement. The third part is to introduce the design and manufacture of the Nano-Skin for skin temperature measurement. Experiments were performed to verify the performance of the Nano-Skin in temperature measurement. Overall, the study concludes that Nano-Skin is a promising product for measuring physiological cues on human-machine contact surfaces to detect human state.

Keywords: human-machine contact; human state detection; physiological cues; sensors; MEMS; NEMS.

1. Introduction

Human state is one of the main factors that affect the performance of human-machine systems (Peter and Herbon, 2006). Recognizing human state in a human-machine system is a highly useful way to improve system performance. Human physiological cues and machine dynamic cues are two main categories of cues for human state detection (Fukuda *et al.* 1995, Reynolds 2001). Change of human state induces changes in human physiological cues and results in specific human behavior which will modify machine dynamic cues. Human physiological cues are more direct indexes of human state. Moreover, machine dynamic cues depend on not only human behavior but also the dynamic characteristics and working environment of machines. Human physiological cues are more suitable for human state detection.

Human state can be detected using physiological cues such as heart rate, skin conductance, skin temperature, operating force, blood alcohol concentration, sweat rate, and electromyography. **Heart rate (HR)** is the number of heart beats per minute. **Heart rate variability** (HRV) is the variation in beat-to-beat intervals. Generally, anger, fear, and sadness induce a larger increase in HR than disgust

---

and neutrality (Gross and Levenson 1997, Levenson *et al.* 1992). HR during the states of anger or fear is higher than that during happiness (Ekman *et al.* 1983, Vrana 1993). HR reflects a close relationship between anticipated effort and arousal (Smith 1989). HRV is influenced by the sympathetic and parasympathetic vagus nerves (Haag *et al.* 2004). **Skin conductance** describes the ability of human skin to conduct electricity. It is a promising and non-invasive physiological measure of autonomic nervous system activity (Cacioppo and Tassinary 1990). Usually, fear and disgust produce larger skin conductance than happiness (Lanzetta and Orr 1986). Sadness does not change skin conductance (Gross and Levenson 1997). Amusement increases skin conductance (Gross and Levenson 1997). Skin conductance also changes with individual levels of overall arousal (Nakasone *et al.* 2005). **Skin temperature** is affected by human state. For example, fear produces a smaller increase in finger temperature than anger (Ekman *et al.* 1983). The finger temperature increases for anger but decreases for fear (Levenson *et al.* 1992). The finger temperature has been involved to detect human state (Sinha and Parsons 1996). In order to operate machines, humans apply an appropriate **operating force** on control devices. The operating force may be increased when humans are nervous and tense, and be decreased when humans are drowsy or fatigued. Human operating force is a useful cue for human state detection (Chieh *et al.* 2003, Bekiaris and Nikolaou 2004). **Blood alcohol concentration (BAC)** represents the amount of alcohol in a person's bloodstream (NIAAA, 2010). Alcohol intake significantly impairs human abilities and degrades human performance (Cherry *et al.* 1983, Kim *et al.* 2007). For example, major driving-related skills were impaired when a driver's BAC was larger than 0.02% (Moskowitz *et al.* 2000). Monitoring BAC is highly relevant to detect human state (Leng and Lin 2010b). **Sweat rate** is the amount of sweat produced per unit time. Human sweat rate increases with higher exercise intensity (Buono and Connolly 1992). Sweat rate is also a useful cue to evaluate human mental stress (Shamsuddin and Togawa 1996). The **electromyography (EMG)** is a sensing method that detects the bioelectric potentials associated with muscle activity. It is suitable for assessing human stress levels and drivers' fatigue (Picard and Healey 1997, Katsis *et al.* 2004). So far, most methods of human state detection employ multiple physiological cues, and are multimodal because multimodal methods can achieve higher recognition accuracy (Anolli *et al.* 2005). It is feasible to detect human state using human physiological cues. One critical step is continuously measuring human physiological cues without disturbing human behavior and state.

In human-machine systems, the physiological measurement may use contact technologies or non-contact technologies (Lin 2011, Schuller *et al.* 2004). Contact technologies require physical human-machine contact; whereas non-contact technologies do not. Contact technologies can achieve a larger signal-to-noise ratio, higher robustness to disturbances, and lower energy consumption, and are preferred in non-intrusive physiological measurement. Human-machine systems involve usually dynamic human-machine contact, e.g., the contact between a driver's palms and the steering wheel. The location and area of human-machine contact may frequently change. It is a challenge to ensure the consistency and continuity of physiological measurement through dynamic human-machine contact, and requires new methods in the area of sensing (Lin *et al.* 2007).

Researchers have found that nature has evolved to offer diverse, impressive, sensitive, and reliable sensing systems for creatures. The mechanism of natural sensing systems is useful to improve the contact technologies for the physiological measurement in dynamic human-machine contact. Human skin consists of two layers, the epidermis and dermis (Tobin 2006). The epidermis is the external layer of keratinizing stratified epithelium. The dermis is a layer of connective tissue beneath the epidermis, and contains a dense network of sensory receptors. The receptor network involves

several types of receptors for different sensations such as touch and pain. The receptor network supports the distributed sensing function of human skin. Researchers recently paid more attention on developing "sensing skin" to enhance the sensing capability of machines (Lumelsky *et al.* 2001, Leng and Lin 2010a), e.g., a sensing skin for monitoring structural health (Lynch and Loh 2009), an infrared-based sensitive skin for planning motion in uncertain environment (Um *et al.* 1998), and a capacitance-based sensitive skin for measuring the distributed pressure on lower limb prosthetic devices and healthcare robots (Rowe and Mamishev 2004, Connolly 2009). These sensing skins expand the sensing capability of machines from a few points to a surface.

Human skin presents an appropriate approach to ensure the consistency and continuity of physiological measurement in dynamic human-machine contact. The receptor network of human skin involves many receptors that are connected with the central nervous system via nerves. The receptor network can be modeled using a star network (Fig. 1). Mimicking the receptor network of human skin, an intelligent sensor array is proposed to address the challenges of physiological measurement in dynamic human-machine contact. An intelligent sensor array involves a microcontroller and many sensors (Fig. 1). All sensors connect with the microcontroller that acquires and processes the signals of sensors. When any one of the sensors is touched by humans, human physiological cue will be measured. This kind of intelligent sensor array can be built into a sensing skin (Fig. 2). The sensing skin has three layers, the substrate, the functional layer, and the protective layer. The functional layer involves sensors, a special integrated circuit (*IC*), and interconnections between the sensors and special *IC* (Fig. 2). The sensors are divided into many sensor groups which are evenly distributed on the substrate. Each sensor group includes a heart rate sensor (HR), a sweat rate sensor (SR), a skin temperature sensor (TE), a gripping force sensor (GF), an alcohol sensor (Al), a skin conductance
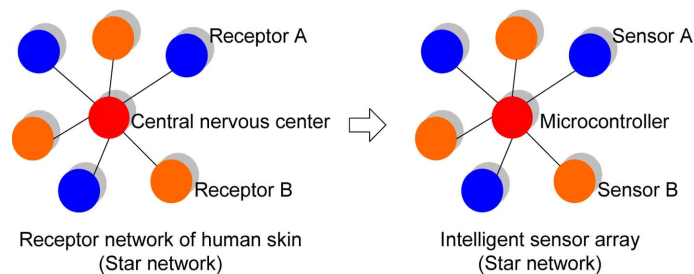

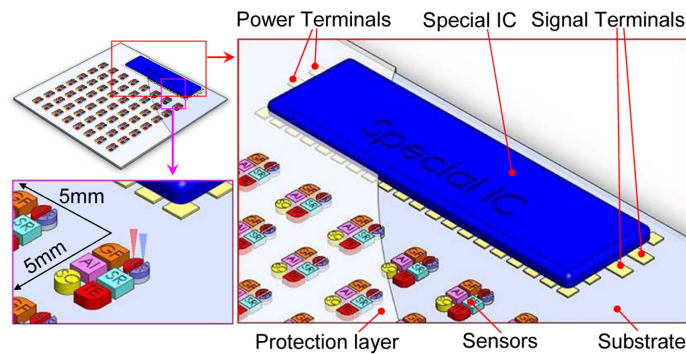Fig. 1 The receptor network of human skin and an intelligent sensor array

Fig. 2 "Nano-Skin" conceptual design

electrode (SC), and an EMG electrode, etc. The heart rate sensor involves a light emitter and detector. The light emitter emits infrared light to illuminate the skin. The reflected infrared light is modified by the perfusion of blood in the skin, which changes the conductivity of the light detector. The skin temperature sensor is a resistance temperature detector. The pressure sensor is a piezo-resistive sensor, and is used to measure human operating force. The sweat rate sensor is a humidity sensor. The alcohol sensor changes resistance with the alcohol concentration of human sweat. The skin conductance and EMG electrodes are good conductors, and are used to measure skin conductance and EMG, respectively. The outputs of these sensors are all resistive changes, and can share one signal conditioning module. The special *IC* is employed to (1) supply appropriate power to the sensing skin, (2) perform the signal acquisition and signal conditioning, and (3) transmit the signals to upper-level computers. The conceptual design of the sensing skin in Fig. 2 involves 56 sensor groups in 7 rows and 8 columns. Each sensor group occupies a 5 mm×5 mm square. A human finger can simultaneously touch at least two sensor groups as human fingers has a diameter of 11.95 mm~ 22.33 mm, according to the US ring size chart.

Manufacturing the sensing skin in Fig. 2 includes mainly preparing the substrate, building the interconnections between sensors and special *IC*, depositing sensing materials, and applying the protective coating layer. When the interconnections are prepared, the sensing skin is covered by the deposition mask #1 for depositing sensing material #1 (Fig. 3). After deposition, mask #1 is removed. The sensing material #1 is left at the desired locations on the substrate to build sensor #1. Similarly, the sensing material for sensor #2 is deposited using deposition mask #2. This process can be repeated to deposit more sensing materials. The sensor shape depends on the deposition mask. The sensor thickness increases with longer deposition time. The special *IC* is a customized *IC*. Its manufacturing will not be discussed in this study.

The sensing skin in Fig. 2 involves six kinds of sensors. The skin temperature sensors do not suffer from cross interferences, whereas the other sensors respond to cross interferences such as the change of temperature. The skin temperature sensors produce signals not only for measuring skin temperature but also for calibrating the outputs of the other sensors of the sensing skin. The skin temperature sensors should be firstly built on the sensing skin and then be evaluated. This paper is focused on developing a bio-inspired sensing skin to measure human skin temperature from human-machine contact surfaces for human state detection. The sensing skin should achieve the safety to humans and the high precision in skin temperature measurement, and involve a dense sensor network to consistently and continuously detect physiological cues in dynamic human-machine contact. It is flexible, and can be attached to curved machines surfaces for diverse applications. The new sensing system is called "Nano-Skin" in this research as it uses nanotechnologies and borrows the sensing mechanism of human skin.
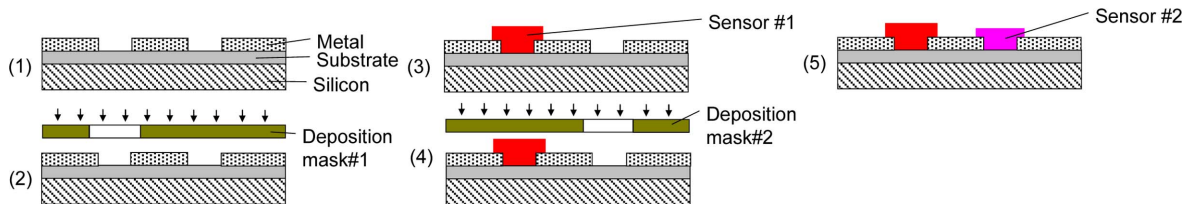

Fig. 3 Deposit sensing materials using deposition masks

2. Sensing technologies for skin temperature

People have developed many technologies for temperature measurement. Common temperature sensors are widespread in the industry field. Their working principles include the thermo-resistive effect, thermoelectric effect, piezoelectric effect, P-N junction, and optical transducer. Thermo-resistive effect means that the resistivity of materials, $\rho_{resistivity}$, changes with ambient temperature, T, as

$$\rho_{resistivity} = \rho_{resistivity-ref} \, [1 + \alpha_{temp} \, (T - T_{ref})] \text{(Fraden 2004)} \tag{1}$$

where $\rho_{resistivity-ref}$ is the resistivity of thermo-resistive materials at a reference temperature T_{ref}. α_{temp} is the temperature coefficient of resistance (TCR). Thermo-resistive sensors usually involve three categories: (1) resistance temperature detectors (RTD) are usually produced using metals or alloys. The popular materials for RTD are platinum and its alloys because they have expectable output and good stability. Most RTDs have a positive temperature coefficient of resistance; (2) silicon resistive sensors are built employing bulk silicon. Pure silicon has initially negative temperature coefficient of resistance. After being doped with an impurity, the silicon shows positive temperature coefficient of resistance in a specific temperature range. Silicon resistive sensors usually have good linearity and good stability; (3) thermistors are made from metal oxides. Thermistors with a negative temperature coefficient are called NTC thermistors, whereas those with positive temperature coefficients are called PTC thermistors. Most thermistors have a nonlinear output and good stability. Thermoelectric effect refers to the conversion between temperature change and electric voltage. Two different metal wires (A and B) which are coupled generate an open-circuit voltage when both their junctions are in different temperatures. The temperature difference of both junctions determines the voltage. Thermoelectric sensors have a linear output and require a "cold" junction in a precisely determined temperature. The piezoelectric effect of some materials is temperature dependent. For example, change in the oscillating frequency of quartz crystal Δf_{quartz} has

$$\frac{\Delta f_{quartz}}{f_{calibrate}} = a_0 + a_1 \Delta T + + a_2 \Delta T^2 + a_3 \Delta T^3 \tag{2}$$

where ΔT is the temperature change, $f_{calibrate}$ is the calibrating frequency, and a_0, a_1, a_2, a_3 are coefficients (Fraden 2004). The frequency shift reflects the temperature though their relation is not linear. PN-junctions of semiconductors have a remarkable thermal dependence. Being supplied constant current, the junction outputs a voltage which is a function of its temperature. Semiconductor PN-junction sensors have good linearity, quick response and strong robustness though it can measure only low temperatures in a limited range (the typical range is -55°C~ + 150°C). Furthermore, optical methods are employed to measure temperature. Optical temperature sensors consist of (1) thermal infrared detectors. Their sensing element responds to electromagnetic radiation in the infrared range. They involve two types, passive and active. Passive infrared detectors can convert incoming radiation to heat. Active infrared detectors emit thermal radiation to measured objects and measure heat loss in the form of thermal radiation. (2) Fluoroptic sensors employ a special phosphor compound which emits fluorescent signals due to light excitation. The response pulse shape of the fluorescent signal is then used to determine temperature; (3) Interferometric sensors employ two light beams: a reference beam and a detecting beam. Compared to the reference beam, the detecting

beam travels through a temperature sensitive medium and is somewhat delayed depending on the medium temperature; and (4) Thermochromic solution sensors show different spectral absorptions for specific temperatures.

MEMS based temperature sensors have also been developed (Xiao *et al.* 2005). These sensors employ sensing principles such as the thermo-resistive effect (Lv *et al.* 2007), Fabry-Perot Micro-Opto-Mechanical Device (FPMOD) (Nieva *et al.* 2006). The FPMOD based MEMS sensor has an optical cavity between a silicon substrate and a silicon nitride film in the form of a cantilever beam. When a monochromatic light source illuminates the FPMOD, the deflection of the beam with respect to the substrate can be measured using Fabry-Perot interferometry to detect the measurands. MEMS sensors are measured in micrometers, and are much smaller than common sensors. The reduction in size increases the sensitivity and decreases the energy-consumption of the sensors.

Nano temperature sensors usually employ the thermal effect of nano materials whose resistance changes with ambient temperature. The thermal nano materials can be metals such as tungsten. The focused-ion-beam chemical vapor deposition (FIB-CVD) of tungsten over an atomic force microscope (AFM) cantilever has a positive temperature coefficient of resistance (El-Shimy *et al.* 2006). The thermal nano material can also be made of nonmetals such as carbon nanotubes. Carbon nanotubes that laterally grow between two electrodes show a linear relation between resistance and ambient temperature (Gau *et al.* 2005, Kuo *et al.* 2007). Nano sensors are in nano-sizes, and have a large surface to volume ratio. Their nano-sizes decrease the input signal intensity required for nano sensors to respond. The large surface to volume ratio enhances interactions between nano sensors and measurands (Traversa *et al.* 2000, Cortie *et al.* 2006).

Measuring human skin temperature for human state detection has special considerations and requirements. Few of current temperature sensors are suitable for this kind of temperature measurement. In human-machine systems, the Nano-Skin operates in the space where humans work. The Nano-Skin temperature sensors will come into close contact with human skin which possibly bears sweat, machine oil, soy sauce, coffee, etc. The Nano-Skin temperature sensors require stability against chemicals found on human skin. The Nano-Skin temperature sensors experience human skin temperature and possible extreme temperatures from the working space. For example, the temperature in a vehicle may reach +60°C or higher in the summer, and be 0°C or lower in winter. The sensors should have good precision in human skin temperature measurement, and work well under all these temperatures. A Nano-Skin on machine surfaces may be applied an operating force by humans. The Nano-Skin temperature sensors should work well under human operating force, and be strong enough to withstand the force. Moreover, the physiological signals on human skin are very weak. Acquiring the signals needs sensors with high sensitivity. The response of sensors will be quick to monitor human state in real time. Building a dense sensor network needs small sensors.

In addition, the skin temperature measurement can not be aware by measured humans, and affect human state. Current temperature sensors are unable to be bent and stretched because they are inflexible, whereas the Nano-Skin is able to. Bending and stretching will not affect the function and performance of the Nano-Skin that is inherently flexible. It is easy to attach the Nano-Skin to curved machines surfaces. Humans may not feel the existence of the Nano-Skin. The effect of using Nano-Skin to human state is greatly decreased. Moreover, measuring human skin temperature for human state detection requires the safety of temperature sensors to humans because skin temperature sensors will directly and continuously contact with human bodies. The safety of most current

temperature sensors to humans was not evaluated, and was not determined. Using the Nano-Skin will be safe to humans. Furthermore, human-machine interaction is usually dynamic. A dense sensor network will be placed on machine surfaces to continuously acquire human skin temperature from human-machine contact surfaces. Establishing this kind of network is difficult for current temperature sensors because (1) the sensor sizes are large. The sensors can not be placed very close; and (2) the sensors are independent from the reading circuits. The interconnections between sensors and reading circuits require extra work, and are mass. This is easy for the Nano-Skin because the Nano-Skin is embedded a dense temperature sensor network. It is worthy to develop a Nano-Skin to monitor skin temperature on human-machine contact surfaces for human state detection.

3. Design and manufacture of the nano-skin for skin temperature measurement

A Nano-Skin for skin temperature measurement was designed and manufactured (Fig. 4). The Nano-skin does not include a special *IC*. Its substrate is employed to support and fix the sensors and interconnections. The substrate is the main component for withstanding external forces. The substrate strain will apply a strain to the sensors and interconnections. If the substrate strain is large, the sensors and interconnections may be broken. The substrate needs good stability under forces. Moreover, the substrate requires high insulating capability because the Nano-Skin temperature sensors and interconnections are built directly on the substrate. The substrate will be flexible to be bent to match curved surfaces. Parylene has a Young's modulus of 2.41~2.76 GPa, a tensile strength of 48.26~75.83 MPa, and a dielectric constant of 3.15. It is flexible, and is proved to be safe to humans. Parylene is an appropriate material for the substrate of the Nano-Skin. A parylene film with a thickness of 10 um was chosen for the Nano-Skin substrate. In addition, platinum is usually employed to produce temperature sensors. It is safe to humans, and does not impair human health. Platinum was chosen to build the Nano-Skin temperature sensors. The Nano-Skin has 9 platinum thermometers with diameters of 5.95 mm, 3.86 mm, 2.82 mm, 2.36 mm, 2.03 mm, 1.78 mm, 1.60 mm, 1.40 mm, and 1.32 mm, respectively. The rectangles along the periphery are the copper pads for connecting data acquisition systems. The interconnections between the sensors and pads are made of copper. The thickness of the sensors, pads, and interconnections is 150 nm. The Nano-Skin was manufactured following the process in Table 1. The Nano-Skin was not covered by a protective layer in order to test its performance in later experiments.
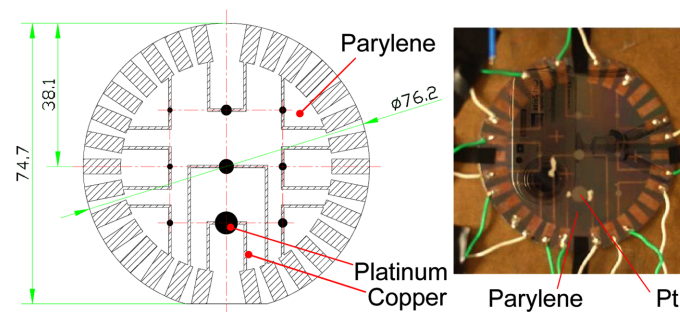

Fig. 4 The Nano-Skin for skin temperature measurement (Left: the engineering drawing and Right: the prototype on a 3" silicon wafer)

Table 1 Manufacturing process of Nano-Skin for skin temperature measurement

No.	Description	Illustration	Details
1	Clean a 3" silicon wafer.	Silicon	Use piranha solution.
2	Spin and coat a PMMA layer.	PMMA	Thickness: 150 nm.
3	Deposit a Parylene layer.	Parylene	Thickness: 10 um.
4	Spin and coat a photo-resist layer.	Photoresist	Use Microposit S1813 photo resist; Thickness: 150 nm.
5	Pattern the photo-resist layer.	Lithograph mask A	Use lithograph mask A. Exposure time: 7 seconds.
6	Develop the photo-resist layer.	Developed photoresist	Use Microposit MF-319 developer.
7	Deposit a copper layer.	Copper	Use the MRC 8667 Sputtering machine.
8	Lift off the copper layer.	Interconnection	Use acetone to remove S1813.
9	Deposit Pt using an e-beam evaporator.	Deposition mask A / Pt	Use the MDC E-beam evaporator and the deposition mask A.
10	Peel off the Nano-Skin from the wafer	Pt	Dip in acetone to dissolve the PMMA.

4. Experiments of the nano-skin for skin temperature measurement

4.1 Experiment apparatus

Besides a Nano-Skin for skin temperature measurement, the experiment apparatus included interface circuits, a USB6218, a computer, a stopwatch, a power supply, a fan heater, a type K thermocouple, a multimeter, a Pt1000Ω thermometer, and an adiabatic board (Fig. 4). The Nano-Skin has 9 platinum temperature sensors (Table 2). Three of them did not work because their resistances were not stable at room temperature. The other 6 sensors show stable resistances at room temperature, and worked well. Their resistive changes in experiment temperatures were measured and then compared to that of the Pt1000Ù. The resistances of the 6 Nano-Skin sensors and the Pt1000Ω were monitored using Wheatstone bridges of which the signal was amplified using an instrumentation amplifier, AD623. Seven interface circuits were prepared for the 6 Nano-Skin sensors and the Pt1000Ω Their signals were acquired and digitized with a sampling frequency of 500 Hz per channel using the NI-USB6218. The fan heater was used to blow hot air to apply temperatures to the sensors. The temperatures applied on the sensors depended on the distance between the fan heater and Nano-Skin (i.e., the D in Fig. 5). A shorter distance resulted in a higher temperature. The experiment temperature was monitored using a type K thermocouple and a multimeter. It was found that the fan heater requires 30 seconds after being started to produce hot air flow with stable temperature. In order to generate the right experiment temperature, the adiabatic board was placed between the Nano-Skin and fan heater to cut the pathway of hot air till the hot air flow temperature became stable.

Table 2 Parameters of the 9 platinum temperature sensors of Nano-Skin

Sensor No.	Diameter (mm)	Resistance in 19ºC (Ω)	Memo	Sensor No.	Diameter (mm)	Resistance in 19ºC (Ω)	Memo
1	5.95	33.0	Tested	N/A	1.78	unstable	N/A
2	3.86	unstable	N/A	6	1.60	9.6	Tested
3	2.82	16.5	Tested	7	1.40	4.6	Tested
4	2.36	unstable	N/A	8	1.32	2.1	Tested
5	2.03	12.5	Tested	Pt1000Ω	N/A	1086	Tested

4.2 Design of experiments

The experiments are to find whether there is significant difference between the resistive changes, response times, and recovery times of the 6 Nano-Skin sensors and those of Pt1000Ω. The experiment factor is the temperature sensor, and has 7 levels: Nano-Skin sensor #1, #3, #5, #6, #7, and #8, and Pt1000Ω. Nine temperatures (e.g., 19ºC, 23ºC, 26ºC, 30ºC, 33ºC, 34ºC, 37ºC, 41ºC, 45ºC, and 48ºC) were produced for the experiments, and involved the typical range of human skin temperature. The voltages of the 7 sensors are simultaneously measured at each experiment temperature. The experiment procedure was (1) the room temperature was measured using the type K thermocouple and multimeter. The voltages of the 7 temperature sensors were acquired for one minute; (2) the fan heater was located with a specific distance from the Nano-Skin to prepare applying the temperature, 37ºC, to the 7 sensors; (3) the adiabatic board was placed between the Nano-Skin and fan heater. The fan heater was started as soon as the stopwatch starts timing at 0 seconds; (4) acquiring the voltages of the temperature sensors began at 30 seconds. The adiabatic board was removed at 32 seconds; (5) the fan heater was stopped at 150 seconds. Simultaneously, the adiabatic board was placed again between the Nano-Skin and fan heater; (6) acquiring the voltages of 7 sensors was continued till 270 seconds; (7) temperatures 48ºC, 41ºC, 23ºC, 34ºC, 30ºC, 45ºC, 33ºC, and 26ºC were successively applied to the 7 sensors by relocating the fan heater. Then steps (3)-(6) were repeated; (8) steps (2)-(7) were repeated another 9 times. In each replication, the order of applying 9 temperatures was randomized.

4.3 Experiment results

The experiments produced 90 data files. In order to analysis the experimental data, a MATLAB program, program-A, was established to read the data file, filter the noise, calculate the sensor
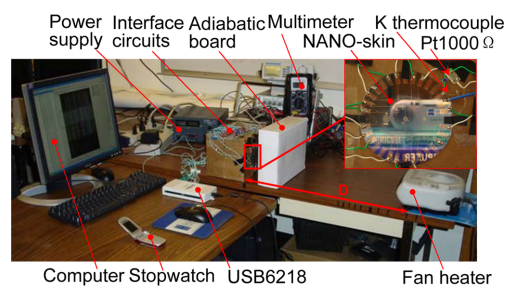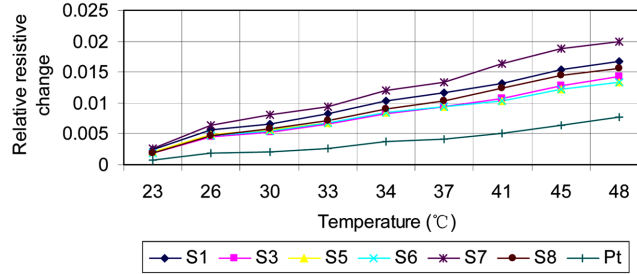

Fig. 5 Experimental apparatus

Fig. 6 $\Delta R_{relative}$ of the Nano-Skin sensors #1,#3, #5, #6, #7, #8 and Pt1000Ω at 9 temperatures

resistances, and then obtain the resistive changes, response times, and recovery times of the 7 sensors at the 9 temperatures. In each experiment, the initial resistance of a sensor, R_{ave_0}, was the average value of the resistances of the sensor in 30~32 seconds. The resistance of the sensor for experiment temperature R_{ave_1} was the average value of the sensor resistances in the 90~150 second time period. The relative resistive change of the sensor at a temperature is $\Delta R_{relative} = (R_{ave\_1} - R_{ave\_0}) / R_{ave\_0}$. The sensor response time, $T_{response}$, is the period from the time a temperature is applied to the time that the sensor achieves the resistance R_{ave_1}. The recovery time of the sensor, $T_{recovery}$, is the period from the time the temperature is removed to the time that the sensor recovers to the resistance R_{ave_0}. Another MATLAB program, program-B, used the analysis of variance (ANOVA) to compare the $\Delta R_{relative}$, $T_{response}$, and $T_{recovery}$ of the 6 Nano-Skin sensors with those of Pt1000Ω at each temperature.

Fig. 6 describes the relative resistive changes of the 6 Nano-Skin sensors and Pt1000Ω at 9 temperatures. Table 3 shows the ANOVA (significance level $\alpha = 0.05$) result of comparing the $\Delta R_{relative}$ s of the 6 Nano-Skin sensors with that of Pt1000Ω at the 9 temperatures. It was verified that $\Delta R_{relative}$ s of the 6 Nano-Skin sensors are significantly different from the $\Delta R_{relative}$ of PT1000Ω at the 9 experiment temperatures. The 6 Nano-Skin sensors are able to produce larger relative resistive changes for same temperature change than PT1000Ω.

The response times of the 6 Nano-Skin sensors and Pt1000Ω at 9 temperatures are recorded in Fig. 7. The ANOVA (significance level $\alpha = 0.05$) result of comparing the response times of the 7 sensors at 9 temperatures are listed in Table 4. There is no significant difference between the response times

Table 3 ANOVA ($\alpha = 0.05$): compare $\Delta R_{relative}$s of 6 sensors with that of PT1000Ω at 9 temperatures

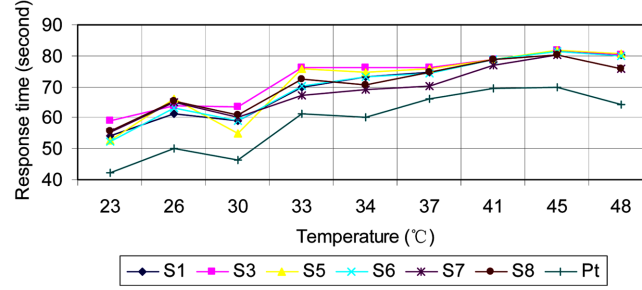| Temperature		P-Value					
	Sensor	Sensor#1	Sensor#2	Sensor#5	Sensor#6	Sensor#7	Sensor#8
23°C		1.34E-05	0.000809	6.84E-05	9.54E-05	2.78E-05	0.000277
26°C		1.37E-08	1.74E-06	1.05E-07	2.39E-07	5.19E-09	4.36E-07
30°C		1.46E-07	1.04E-05	1.83E-06	2.45E-06	9.95E-09	7.33E-07
33°C	PT1000 Ω	1.24E-09	4.71E-07	6.25E-08	6.73E-08	2.80E-11	2.68E-08
34°C		7.50E-08	9.11E-06	5.28E-06	5.03E-06	3.62E-09	9.18E-07
37°C		1.26E-08	2.08E-06	1.44E-06	1.11E-06	6.75E-10	1.93E-07
41°C		5.55E-06	2.75E-04	4.33E-04	4.53E-04	9.93E-08	1.31E-05
45°C		1.37E-08	1.74E-06	1.05E-07	2.39E-07	5.19E-09	4.36E-07
48°C		5.99E-06	2.04E-04	9.37E-04	1.06E-03	2.19E-07	2.97E-05

Fig. 7 $T_{response}$ of the Nano-Skin sensors #1,#3, #5, #6, #7, #8 and Pt1000Ω at 9 temperatures

Table 4 ANOVA ($\alpha = 0.05$): comparing $T_{response}$s of 6 sensors with that of PT1000Ω at 9 temperatures

Temperature		P-Value					
	Sensor	Sensor#1	Sensor#2	Sensor#5	Sensor#6	Sensor#7	Sensor#8
23ºC		5.37E-02	0.005788	1.87E-01	1.92E-01	8.54E-02	0.083183
26ºC		2.12E-01	1.23E-01	7.35E-02	1.45E-01	8.79E-02	7.57E-02
30ºC		1.07E-01	1.88E-02	2.64E-01	1.00E-01	7.42E-02	6.26E-02
33ºC	PT1000 Ω	1.84E-01	1.42E-02	1.99E-02	1.70E-01	4.17E-01	6.33E-02
34ºC		2.77E-02	8.99E-03	1.40E-02	2.66E-02	1.14E-01	5.11E-02
37ºC		8.44E-02	3.00E-02	4.23E-02	9.07E-02	4.49E-01	7.37E-02
41ºC		5.48E-02	5.44E-02	5.88E-02	6.21E-02	1.47E-01	5.94E-02
45ºC		4.40E-02	4.64E-02	4.62E-02	5.34E-02	7.78E-02	7.61E-02
48ºC		1.24E-02	1.29E-02	1.13E-02	1.56E-02	9.50E-02	9.65E-02

of the Nano-Skin sensors #7 and #8 and that of PT1000Ω at the 9 temperatures. The Nano-Skin sensors #1 and #6 had the same response times as PT1000Ω at temperatures 6 and 7, respectively. However, the Nano-Skin sensors #2 and #5 showed significantly different response times from PT1000Ω at most experiment temperatures. Smaller Nano-Skin sensors have the potential to respond as quickly as PT1000Ω.

The recovery times of the 7 sensors are illustrated in Fig. 8. The ANOVA (significance level $\alpha = 0.05$) of recovery time produced the results in Table 5. It was verified that (1) the recovery time of the Nano-Skin sensors #7 and #8 is statistically equal to that of PT1000Ω at the 9 temperatures;
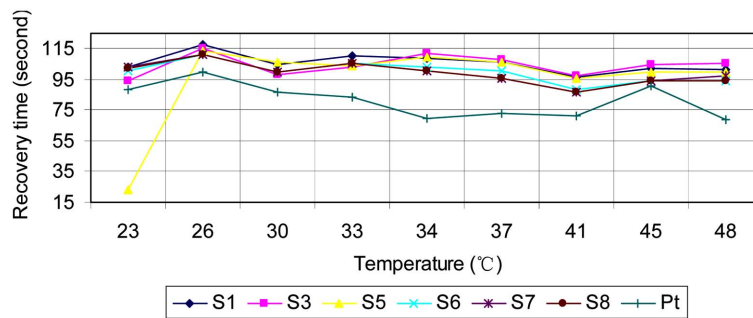

Fig. 8 of the Nano-Skin sensors #1,#3, #5, #6, #7, #8 and Pt1000Ω at 9 temperatures

Table 5 ANOVA ($\alpha = 0.05$): comparing $T_{response}$s of 6 sensors with that of PT1000Ω at 9 temperatures

Temperature	Sensor	P-Value					
		Sensor#1	Sensor#2	Sensor#5	Sensor#6	Sensor#7	Sensor#8
23 ºC	PT1000 Ω	2.87E-01	0.69339	1.21E-03	3.78E-01	3.10E-01	0.31737
26 ºC		2.76E-03	8.18E-03	4.13E-02	6.98E-02	7.09E-02	7.34E-02
30 ºC		2.93E-02	2.49E-01	1.46E-02	8.31E-02	8.31E-02	8.31E-02
33 ºC		2.76E-02	1.62E-01	1.48E-01	5.95E-02	5.97E-02	5.97E-02
34 ºC		2.22E-02	1.44E-02	2.16E-02	4.75E-02	7.38E-02	7.38E-02
37 ºC		4.08E-02	3.19E-02	3.87E-02	8.13E-02	1.75E-01	1.75E-01
41 ºC		5.30E-03	2.75E-03	6.65E-03	4.13E-02	6.92E-02	6.92E-02
45 ºC		5.89E-04	6.62E-04	2.50E-03	2.31E-01	2.31E-01	2.31E-01
48 ºC		4.29E-02	2.63E-02	5.61E-02	1.09E-01	8.23E-02	1.11E-01

(2) In 7 out of 9 temperatures, the Nano-Skin sensor #6 has the same recovery time as PT1000Ω; and (3) the recovery times of the Nano-Skin sensors #1, #2, and #5 are significantly different from that of PT1000Ω at most temperatures. The Nano-Skin sensors #1, #2, and #5 may have longer recovery times than PT1000Ω. The Nano-Skin sensors can achieve similar recovery time to PT1000Ω when their sizes are optimized.

5. Conclusions

Monitoring human state in human-machine systems is highly useful to improve system performance. Physiological cues have more direct and close relationships with human state than machine dynamic cues. It is better to non-intrusively measure human physiological cues from human-machine contact surfaces for human state detection. A Nano-Skin involves a dense sensor network, mimicking human skin, and is a bio-inspired sensing system for human-machine contact based physiological measurement. It is flexible, and can be attached to curved machine surfaces. A Nano-Skin has mainly a flexible substrate, sensors, a special integrated circuit, interconnections, and a flexible protective layer. The sensors are connected with the special integrated circuit via the interconnections. Their signals are acquired, processed, and transmitted using the special integrated circuit. The sensors, special integrated circuit, and interconnections are fixed and packaged between the substrate and protective layer. This study manufactured a Nano-Skin for skin temperature measurement, and then tested its performance. The manufacturing process is feasible and repeatable. The Nano-Skin sensors produced larger relative resistive changes for same temperature change than a PT1000Ω sensor. Depending on their size, the Nano-Skin sensors are able to achieve same response and recovery times as PT1000Ω. It is feasible to use the Nano-Skin to non-intrusively measure human physiological cues on human-machine contact surfaces for human state detection.

In the future, the Nano-Skin will be extended to include more transducer elements to measure more human physiological cues.

Acknowledgements

References

Anolli, L., Mantovani, F., Mortillaro, M., Vescovo, A., Agliati, A., Confalonieri, L., Realdon, O., Zurloni, V. and Sacchi, A. (2005), "A multimodal database as a background for emotional synthesis, recognition and training in e-learning systems", Affective Computing and Intelligent Interaction, *Proceedings of the 1st International Conference*, ACII 2005, Lecture Notes in Computer Science, **3784**, 566-573.

Bekiaris, E.D. and Nikolaou, S.I. (2004), "Towards the development of design guidelines handbook for driver hypovigilance detection and warning - the AWAKE approach", *Proceedings of the 12th IEE International Conference on Road Transport Information & Control*, RTIC 2004.

Buono, M.J. and Connolly, K.P. (1992), "Increases in sweat rate during exercise: gland recruitment versus output per gland", *J. Therm. Biol.*, **17**(4-5), 267-270.

Cacioppo, J.T. and Tassinary, L.G. (1990), "Inferring psychological significance from physiological signals", *Am. Psychol.*, **45**(1), 16-28.

Cherry, N., Johnston, J., Venables, H., Waldron, H., Buck, L. and MacKay, C. (1983), "Effects of toluene and alcohol on psychomotor performance", *Ergonomics*, **26**(11), 1081-1087.

Chieh, T.C., Mustafa, M.M., Hussain, A., Zahedi, E. and Majlis, B.Y. (2003), "Driver fatigue detection using steering grip force", *Proceedings of the Student Conference on Research and Development* , SCOReD 2003.

Connolly, C. (2009), "Touch-sensitive skins for Japanese health care robots", *Sens. Rev.*, **29**(2), 104-106.

Cortie, M., Maaroof, A., Mortari, A. and Wuhrer, R. (2006), "Applications of nano- and mesoporous gold in electrodes and electrochemical sensors", *Proceedings of the 2006 International Conference on Nanoscience and Nanotechnology*, ICONN, 524-527.

Ekman, P., Levenson, R.W. and Friesen, W.V. (1983), "Autonomic nervous system activity distinguishes among emotions", *Science*, **221**(4616), 1208-1210.

El-Shimy, H.M.M., Arai, F. and Fukuda, T. (2006), "Three-dimensional nano temperature sensors", *Proceedings of the 6th IEEE Conference on Nanotechnology*, 770-772.

Fraden, J. (2004), Handbook of modern sensors, American Institute of Physics.

Fukuda, J., Akutsu, E. and Aoki, K. (1995), "Estimation of driver's drowsiness level using interval of steering adjustment for lane keeping", *JSAE Review*, **16**(2), 197-199.

Fung, C. and Li, W. (2003), "Ultra-low-power and high-frequency-response carbon nanotube based MEMS thermal sensors", *Proceedings of the IEEE International Conference on Intelligent Robots and Systems*, **3**, 2371-2376.

Gau, C., Chan, C., Shiau, S.H., Liu, C.W. and Ting, S.H. (2005), "Nano temperature sensor using selective lateral growth of carbon nanotube between electrodes", *Proceedings of the 5th IEEE Conference on Nanotechnology*, **1**, 129-132.

Gross, J.J. and Levenson, R.W. (1997), "Hiding feelings: the acute effects of inhibiting negative and positive emotion", *J. Abnormal Psychol.*, **106**(1), 95-103.

Haag, A., Goronzy, S., Schaich, P. and Williams, J. (2004), "Emotion recognition using bio-sensors: First steps towards an automatic system", Lecture Notes in Artificial Intelligence (Subseries of Lecture Notes in Computer Science), v 3068, Affective Dialogue Systems, 36-48.

Katsis, C.D., Ntouvas, N.E., Bafas, C.G. and Fotiadis, D.I. (2004), "Assessment of muscle fatigue during driving using surface EMG", *Proceedings of the IASTED International Conference on Biomedical Engineering*, 259- 262.

Kim, H., Yang, C., Lee, B., Yang, Y. and Hong, S. (2007), "Alcohol effects on navigational ability using ship handling simulator", *Int. J. Ind. Ergonom.*, **37**(9-10), 733-743.

Kuo, C., Chan, C., Gau, C., Liu, C., Shiau, S. and Ting, J. (2007), "Nano temperature sensor using selective lateral growth of carbon nanotube between electrodes", *IEEE T. Nanotechnol.*, **6**(1), 63-69.

Lanzetta, J.T. and Orr, S.P. (1986), "Excitatory strength of expressive faces: effects of happy and fear expressions and context on the extinction of a conditioned fear response", *J. Personality Soc. Psychol.*, **50**(1), 190-194.

Lin, Y. (2011), "Natural contact and non-intrusive sensing of physiological cognitive signals in human-machine interactions", *IEEE Sens. J., Special Issue on Cognitive Sensor Networks*, **11**(3), 522-529.

Leng, H. and Lin, Y. (2010a), "Design and fabrication of a MEMS/Nano-Skin system for human physiological response measurement", *Proceedings of the Sensors and Smart Structures Technologies for Civil, Mechanical, and Aerospace Systems*, San Diego, USA, March.

Leng, H. and Lin, Y. (2010b), "Design and experimental study of the CNT based sensor toward measuring blood alcohol concentration (BAC) with short response delay", *IEEE Sens. J.*, **10**(6), 1091-1097.

Levenson, R.W., Ekman, P., Heider, K. and Friesen, W.V. (1992), "Emotion and autonomic nervous system activity in the Minangkabau of west Sumatra", *J. Personality Soc. Psychol.*, **62**(6), 972-988.

Lin, Y., Leng, H., Yang, G. and Cai, H. (2007), "An intelligent noninvasive sensor for driver pulse wave measurement", *IEEE Sens. J.*, **7**(5), 790-799.

Lumelsky, V.J., Shur, M.S. and Wagner, S. (2001), "Sensitive skin", *IEEE Sens. J.*, **1**(1), 41-51.

Lv, X., Zhang, Z. and Kong, D. (2007), "A catalytic sensor using MEMS process for methane detection in mines", *Proceedings of the 2007 International Conference on Information Acquisition,* ICIA.

Lynch, J.P. and Loh, K.J. (2009), "Bio-inspired sensing skins for civil infrastructure applications", *Proceedings of the International Workshop on Bio-Inspired Sensing and Bio-Inspired Actuation Technology*, Taipei, Taiwan, April.

Moskowitz, H., Burns, M., Fiorentino, D., Smiley, A. and Zador, P. (2000), "Driver characteristics and impairment at various BACs", http://www.nhtsa.dot.gov/people/injury/research/pub/impaired_driving/BAC/impairment. pdf.

Nakasone, A., Prendinger, H. and Ishizuka, M. (2008), "Emotion recognition from electromyography and skin conductance", *Proceedings 5th International Workshop on Biosignal Interpretation (BSI-05)*, Tokyo, Japan.

National Institute on Alcohol abuse and Alcoholism (NIAAA), (2010), "Blood Alcohol Concentration Limits: Operators of Recreational Watercraft", http://alcoholpolicy.niaaa.nih.gov/index.asp?SEC={5D1BAF7B-6855-4584-8829-41F4001C8ACE}&type=BAS_APIS.

Nieva, P., McGruer, N. and Adams, G. (2006), "A multipurpose optical MEMS sensor for harsh environments", 2006 NSTI Nanotechnology Conference and Trade Show - NSTI Nanotech 2006 Technical Proceedings, v 3, 2006 NSTI Nanotechnology Conference and Trade Show - NSTI Nanotech 2006 Technical Proceedings, 419-422.

Peter, C. and Herbon, A. (2006), "Emotion representation and physiology assignments in digital systems", *Interact. Comput.*, **18**(2), 139-170.

Picard, R. and Healey, J. (1997), "Affective wearables", *Proceedings of the 1st Int'l Symposium on Wearable Computers*, 90-97.

Reynolds, C. (2001), The Sensing and Measurement of Frustration with Computers, Master thesis, Massachusetts Institute of Technology, May 2001.

Rowe, G. and Mamishev, A. (2004), "Simulation of a sensor array for multi-parameter measurements at the prosthetic limb interface", *Proceedings of the SPIE - The International Society for Optical Engineering*, v 5394, 2004, Health Monitoring and Smart Nondestructive Evaluation of Structural and Biological Systems III, 493-500.

Schuller, B., Rigoll, G. and Lang, M. (2004), "Speech emotion recognition combining acoustic features and linguistic information in a hybrid support vector machine-belief network architecture", Acoustics, Speech, and Signal Processing, 2004. Proceedings of the IEEE International Conference on Vol. 1, 17-21 May 2004, vol.1, 577-580.

Shamsuddin, A.K.M. and Togawa, T. (1996), "Continuous measurement of sweat electrolyte quantity to evaluate mental stress", *Proceedings fo the Annual International Conference of the IEEE Engineering in Medicine and Biology*, **1**, 38-39.

Sinha, R. and Parsons, O. (1996), "Multivariate response patterning of fear and anger", *Cognition Emotion*, **10**(2), 173-198.

Smith, C.A. (1989), "Dimensions of appraisal and physiological response in emotion", *J. Personality Soc. Psychol.*, **56**(3), 339-353.

Tobin, D.J. (2006), "Biochemistry of human skin - our brain on the outside", *Chem. Soc. Rev.*, **35**(1), 52-67.

Traversa, E., Carotta, M.C. and Martinelli, G. (2000), "Nano-sized semiconducting oxide powders for thick film gas sensors: from powder processing to environmental monitoring devices", *Proceedings of the Materials*

Research Society Symposium, **581**, 121-132.

Um, D., Stankovic, B., Giles, K., Hammond, T. and Lumelsky, V. (1998), "A modularized sensitive skin for motion planning in uncertain environments", *Proceedings of the IEEE International Conference on Robotics and Automation (Cat. No.98CH36146)*, **1**, 7-12.

Vrana, S. (1993), "The psychophysiology of disgust: differentiating negative emotional contexts with facial EMG", *Psychophysiology*, **30**(3), 279-286.

Xiao, S., Che, L., Li, X. and Wang, Y. (2005), "Temperature sensor array based on flexible MEMS skin technology", Guangxue Jingmi Gongcheng/Optics and Precision Engineering, **13**(6), 674-680.